American Journal of Interdisciplinary Research and Development
ISSN Online: 2771-8948
Website: www.ajird.journalspark.org
Volume 10, Nov., 2022

MODELING OF THE "Y" AND "G" CODE TRANSMISSION PROCESS OF THE MICROELECTRONIC CODE TRANSMITTER USING PETRI NETS

Nazirjon Mukramovich Aripov
Doctor of Technical Sciences, Professor, Tashkent
State Transport University. Tashkent

Zafar Fakhridinovich Mirzarakhmedov
Senior Lecturer of the Driver Training Center under the Tashkent
Transport College

Shukhrat Batirovich Djabbarov
PhD, Docent, Tashkent State Transport University. Tashkent

ANNOTATION

Currently, microprocessor, microelectronic systems and devices used in railway automation and remote control systems are widely used. The use of systems and devices for railway automation and remote control, developed on the basis of microelectronics and microprocessor elements, provides an increase in the level of reliability compared to systems based on electromagnetic relays.

In this article, the modeling of transmitter relays designed to transmit the codes generated by the KPTSH transmitter to road traffic lights and locomotive traffic lights in rail chains equipped with auto-blocking systems and automatic locomotive signaling systems at the joint-stock company «Uzbekistan Temir Yollari» is considered.

The process of modeling «Y» and «G» codes (For yellow and green codes) based on Petri net graphs of the newly developed integrated microprocessor code transmitter for the transmission of codes formed in railway automation and telemechanics systems is considered. Time descriptions of transmitter relay pulses and «Y» and «G» codes pulse and interval timing diagrams for transmitter relays. In addition, «Y» and «G» codes have been studied.

Keywords: automatic blocking, locomotive automatic signaling, track circuits, code, processes, anchor, relay, Petri nets, graphs.

One of the most acute scientific problems in the field of railway automation and telemechanics is to ensure the safety level and reliability factor of control systems and equipment, as well as to improve the areas of analysis and synthesis of their work [1-12].

In order to increase the level of safety in the devices and systems of railway automation and telemechanics, multi-channel control methods have been introduced. The basis of these channels is equipment, software and time reserve, and the goal is to create reserves for the safety and stability of elements, to eliminate equipment failures in the system [12-19].

To date, when implementing the same methods of improving safety on railways, the operating conditions of equipment and systems of railways, the development of railways and the speed of trains operating on them are not always taken into account [8].

As a result, the use of only one technical solution to increase the level of security in most cases leads to the fact that software and hardware systems work more than necessary, which reduces the efficiency of work and complicates their structure.

Therefore, it becomes relevant to increase the level of safety in the operation of equipment and systeMS of railway transport, the development and implementation of methods for assessing their impact on the movement of trains and taking into account economic factors.

Petri nets are a tool for implementing the system. The theory of Petri nets makes it possible to model railway automatic and telemechanics systems in a mathematical hypothesis. The theory of Petri nets was developed to model parallel processes in systems.

Petri nets are built on the basis of P processes, T conditional transitions, I input and O output elements of the problem. Input and output functions are interconnected through processes and conditional jumps. This ensures the correspondence of processes and conditional transitions in the structure of Petri nets [17-20].

The difference between pulses and intervals in the transmission of the relay code of TSH transmitters requires the implementation of separate processes for each code in Petri graphs. Based on the generated Petri charts below, the TSH-65 and TSH-2000 relays. Let's get acquainted with the modeling for the code «Y- (for Yellow)».

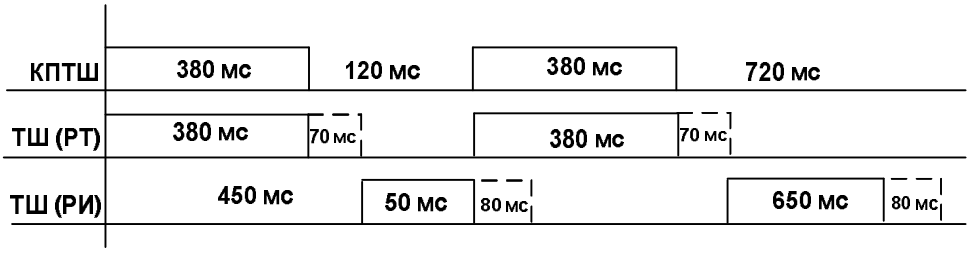

Figure 1. Diagram of the time characteristics of the pulse intervals in the code "Y" for the relay-transmitters TSH-65 and TSH-2000.

Table 1 lists the processes and descriptions of the processes in Petri nets for the code «Y»:

Table 1

Order of proceedings	**Purpose of the procedure**
P1	The supply was given and the impulse started to come.
P 2	During the pulse, the process of raising the armature of the RT relay.
P3	The process of checking the arrival of a pulse for 380 MS.
P4	70 MS to reset the RT relay within the interval after the end of the delay time pulse.
P11	
P5	Dropping of RT relay armature .
P6	Processing interval 50 MS.
P7	Relay armature lifting RI.
P8	The delay in the arrival of the pulse and the armature of the relay RI is 80 MS and the process of the arrival of the pulse is 380 MS.
P13	
P9	Delay time 80 MS for the arrival of the pulse and deactivation of the armature of the relay RI after the process of checking the timeout interval.
P10	Relay armature drop RI
P12	Process arrival interval 650 MS
Order of conditions	**Assigning transition conditions**
t1	Start of pulse reception 0÷380 MS
t2	Checking the transition condition to the interval after the end of the impulse.
t3	After a delay of 70 MS, the armature of the PT relay switches from on to de-energized.
t12	
t4	Checking if the 70 MS delay time expires and the 50 MS interval continues.
t5	Checking the start of the 80 MS delay after the 50 MS interval.
t6	Check pulse arrival for 300 ms.
t7	After a delay of 70 MS, relay RT is de-energized and RI is turned on.
t8	80 MS latency check after 650 MS interval.
t9	Relay RI de-energized.

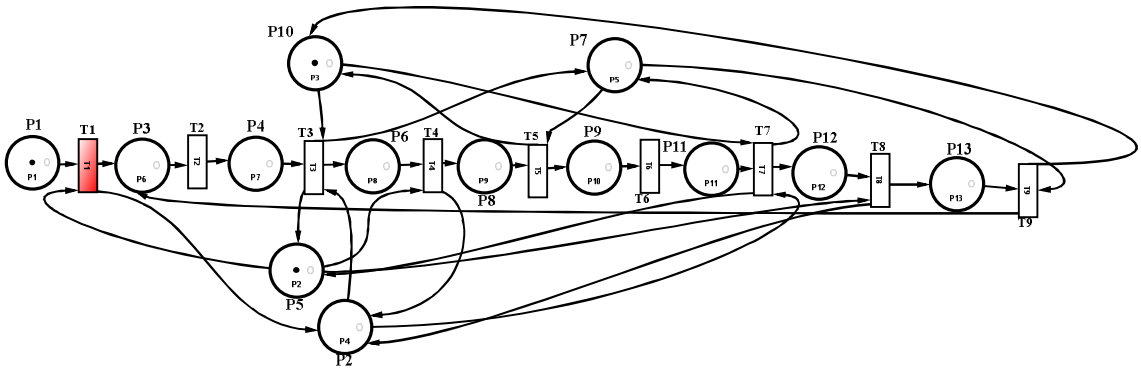

Figure 2. Code "Y" Initial state of the transmitter relay TSH when power is connected Graphical representation of a Petri net

The graph uses state transitions t1, t2, ... and t14 and positions P1, P2 ..... and P16.

In figure 2, when the power is connected and a pulse is input, the P1 chip activates the position. And the transition condition t1 checks the fulfillment of the condition for receiving an impulse within 380 MS, and if the condition is met, outputs O(t1) = {P2, P3} are formed.

These outputs activate the positions shown in Figure 3. As a result of the activation of the process P2 by the transition t1, the relay PT picks up the armature, i.e. it changes to the current state. And process P3 controls the process of receiving a pulse to P2 for 0÷380 MS. After the specified time has elapsed, I(t2)={P3} checks the condition for the beginning of the interval at the end of the input pulse.

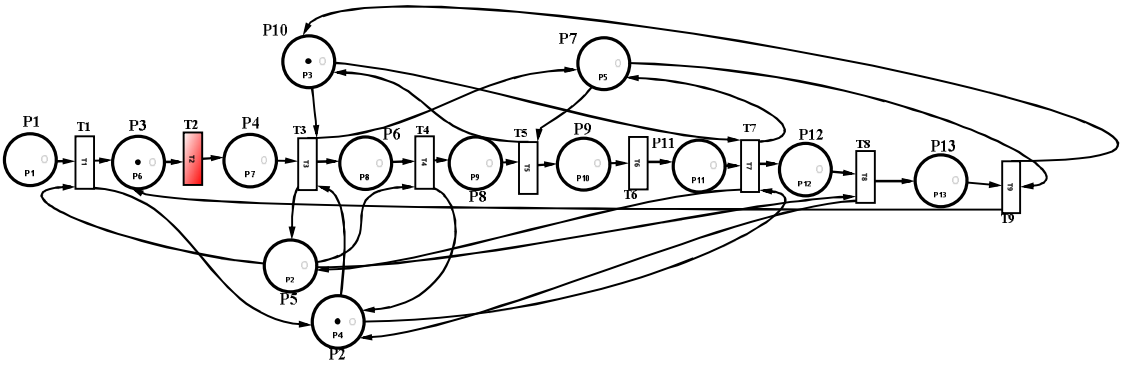

Figure 3. When the power is connected to the relay of the TS transmitter for the code "Y", a pulse with a duration of 0÷380 MS arrives. Representation of the Petri net graph

Checking for another 70 MS delay before the end of the pulse to drop the armature RT is created by activating position P4 (fig. 4).

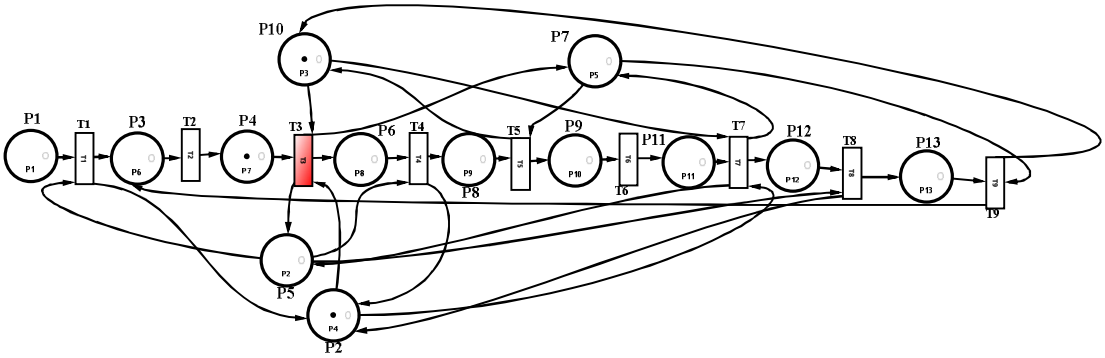

Figure 4. Plot of the Petri net of the 70 MS delay process for checking the drop of the PT armature for the "Y" code when power is applied

After the 70 MS delay time for R4 to de-energize the RT armature, the I(t3)={P4,P10} inputs check that the armature is fully de-energized, that is, the process condition for RT transitioning from the energized state to the de-energized state.

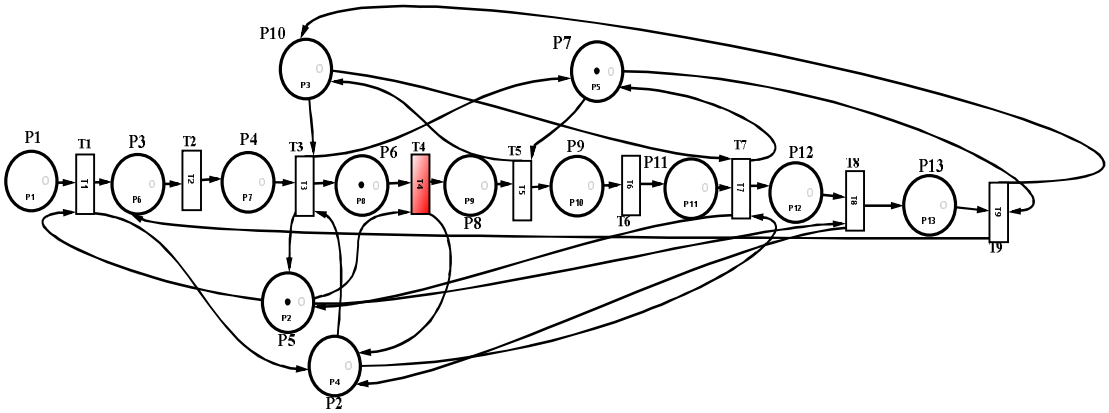

Figure 5. Petri net plot of PT anchor drop and 50 MS interval for code "Y".

In Figure 5, as a result of the output O(t3)={P5}, a chip is generated in process R5, which represents that the RT anchor has dropped. The occurrence of the output O(t3)={P7} is the basis for the transition of the armature RI from the de-energized state to the on state. And the output O(t3)={P6} activates the P6 position, P6 in turn organizes the interval duration process for 50 MS. The sequential occurrence of P4 and P6 processes ensures a total interval of 120 MS. After the process of P6 is completed, we have the output O(t4)={P2} and thus start sending a pulse to start cycle 2.

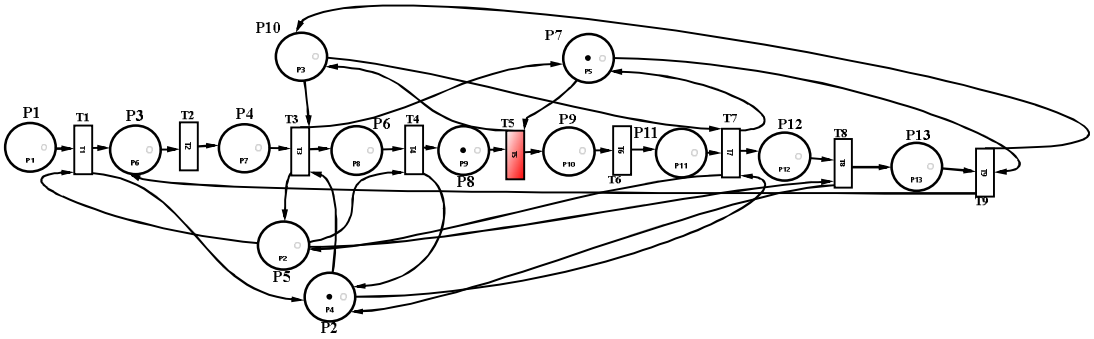

Figure 6. Plot of the Petri net of the 80 MS delay process for checking the drop of the RI armature for the "Y" code when power is applied

I(t5)={P8} checks the start condition after a delay of 80MS after parameter t5 is enabled. When this condition is met, process P8 is activated. Figure 6.

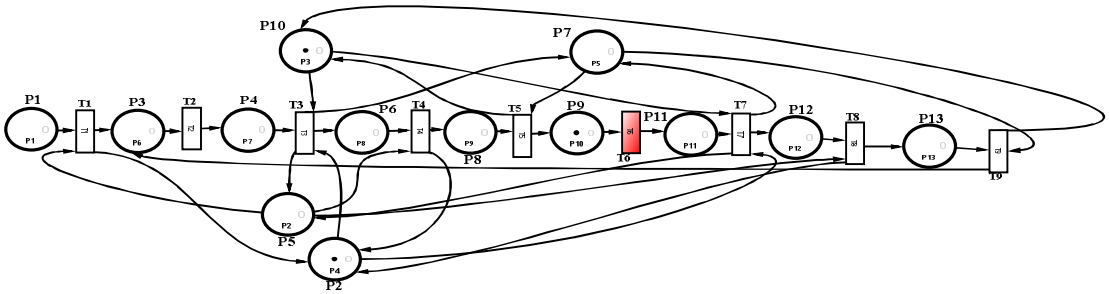

Figure 7. (Image of Petri nets of impulse arrival for 300 MS)

The R9 position is activated by the input I(t6)={P9}. The P9 state represents the arrival of a 300 ms pulse. At the same time, the process of activation also occurs in the P2 state, which means that the RT armature is in a live state.

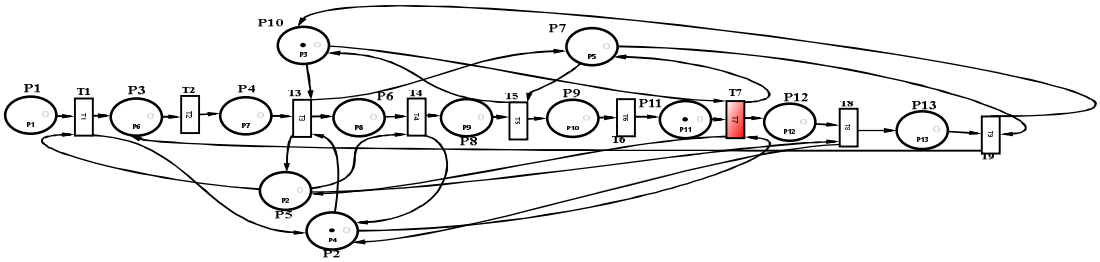

Figure 8. Plot of the Petri net of the 70 MS delay process for checking the drop of the PT armature for the "Y" code when power is applied

(I(t7)={P11} input shows the execution process of the delay time condition for R11 position RT anchor to fall. I(t7)={P10,R11} inputs represent the end of 70 MS delay.)

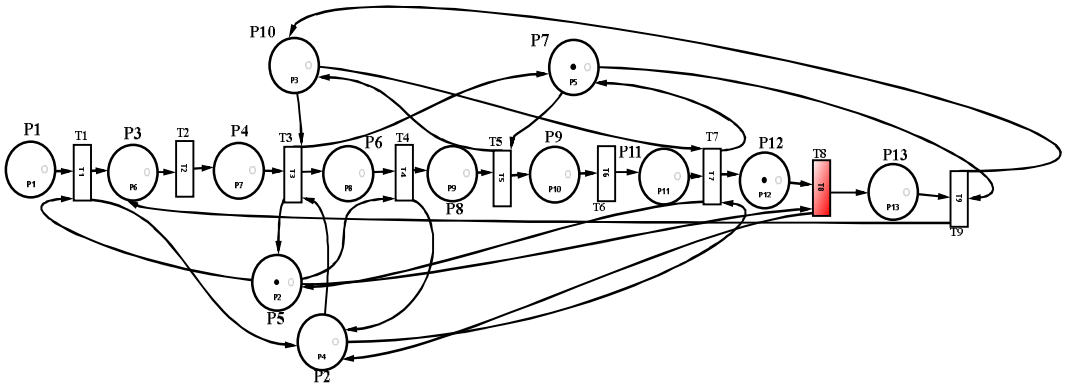

Figure 9. Interval of 650 the code «Y» Petri net chart

(O(t7)={P12} is generated when process R12 is activated, which means that there is an interval of 650 MS.
It is shown that the RT armature switches from the uncurrent state to the current state as a result of the generation of the output O(t8)={P2}.)

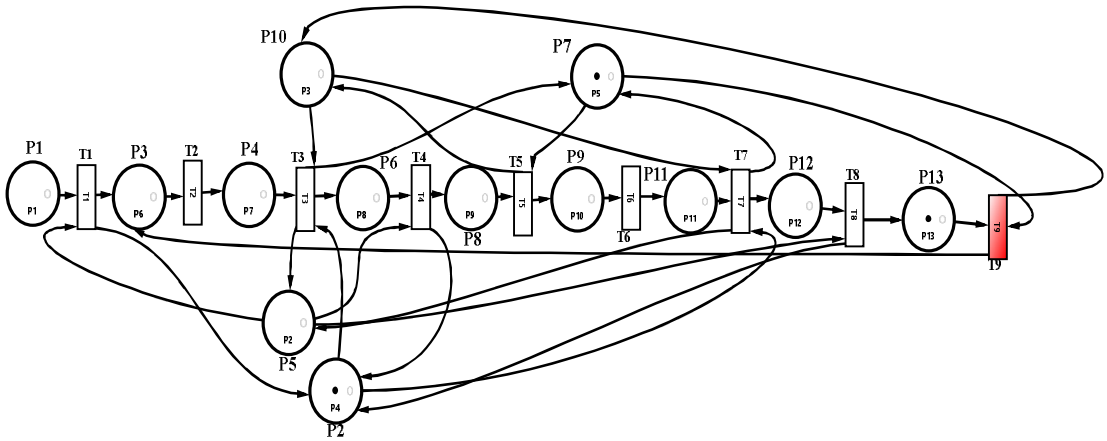

Figure 10. Plot of the Petri net of the 80 MS delay process for checking the drop of the RI armature for the "Y" code when power is applied

Fig. 10 (The fact that we have input I(t7)={P2} means that the pulse start process and the pulse arrival process 380 MS into the cycle are activated.)
As a result of the input I(t9)={P13}, it is expressed that the 80 MS delay process shown in its technical characteristics occurs for the transition of the RI armature from the current state to the non-current state.

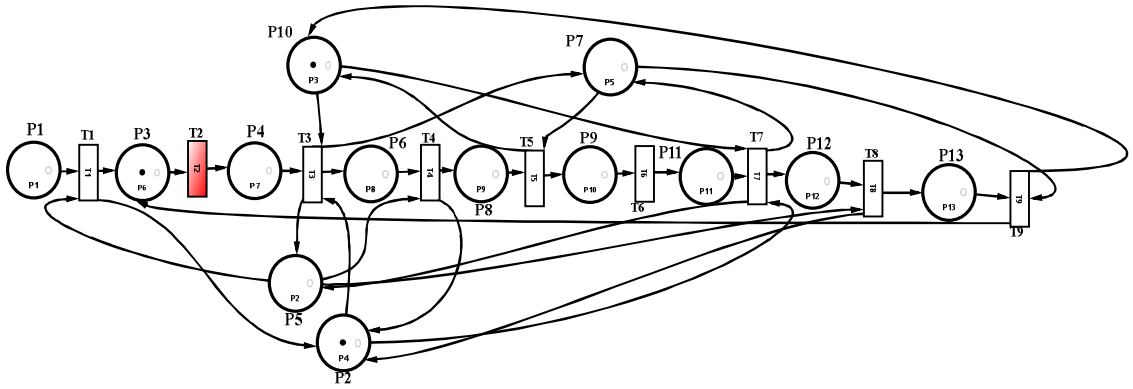

Figure 11. Beginning of the 2nd cycle for the code “Y” Petri net chart

I(t9)={P7,R13} shows that as a result of the fulfillment of the input conditions, RI lowers its anchor through the output O(t9)={P10}, meaning that the interval is over. And through the output O(t9)={P3}, the code "Y" returns to its original state.

These processes will be started again if the code “Y” will not change, and will continue in that order.

Extended input (I) and output (O) functions for the Petri graph in the code “Y” of the TSH-65 relay are presented in Table 2.

Table 2

I(t1) = {P1}	*O(t1)={P2,P3}*
I(t2)={R3}	*O(t2)={P4}*
I(t3)={R2,P4}	*O(t3)={P5}*
I(t4)={P4}	*O(t4)={P6}*
I(t5)={P6}	*O(t5)={P8}*
I(t6)={P5}	*O(t6)={P7}*
I(t7)={P8}	*O(t7)={P9}*
I(t8)={P7,R8}	*O(t8)={P10}*
I(t9)={P9}	*O(t9)={P12}*
I(t10)={P6}	*O(t10)={P11}*
I(t11)={P12}	*O(t11)={P13}*
I(t12)={P11,R12}	*O(t12)={P14}*
I(t13)={P14}	*O(t13)={P15}*
I(t14)={P13}	*O(t14)={P1,R16}*
I(t15)={P15,R16}	*O(t15)={P17}*

Corresponding to the expression in table 2, the expression for matrices 1 and 2 in shape.

$$i_{j\varepsilon} = \begin{cases} 1, agar \rightarrow p_\varepsilon \in P^I t_j \cup t_j \in T^0 p_\varepsilon, \\ 0, agar \rightarrow p_\varepsilon \notin P^I t_j \cap t_j \notin T^0 p_\varepsilon \end{cases}$$

Matrix 1

$I=|t_{\tau\varepsilon}| =$

P1	P2	P3	P4	P5	P6	P7	P8	P9	P10	P11	P12	P13	
1	0	0	0	1	0	0	0	0	0	0	0	0	t1
0	0	1	0	0	0	0	0	0	0	0	0	0	t2
0	1	0	1	0	0	0	0	0	1	0	0	0	t3
0	0	0	0	1	1	0	0	0	0	0	0	0	t4
0	0	0	0	0	0	1	1	0	0	0	0	0	t5
0	0	0	0	0	0	0	0	1	0	0	0	0	t6
0	1	0	0	0	0	0	0	0	1	1	0	0	t7
0	0	0	0	1	0	0	0	0	0	0	1	0	t8
0	0	0	0	0	0	1	0	0	0	0	0	1	t9

Matrix 2

$O=|t_{\tau\varepsilon}| =$

P1	P2	P3	P4	P5	P6	P7	P8	P9	P10	P11	P12	P13	
0	1	1	0	0	0	0	0	0	0	0	0	0	t1
0	0	0	1	0	0	0	0	0	0	0	0	0	t2
0	0	0	0	1	1	1	0	0	0	0	0	0	t3
0	1	0	0	0	0	0	1	0	0	0	0	0	t4
0	0	0	0	0	0	0	0	1	1	0	0	0	t5
0	0	0	0	0	0	0	0	0	0	1	0	0	t6
0	0	0	0	1	0	1	0	0	0	0	1	0	t7
0	0	0	0	0	0	0	0	0	0	0	0	1	t8
0	0	1	0	0	0	0	0	0	1	0	0	0	t9

Below we will get acquainted with how the Petri graphs for the« G - (for grenn)» code are expressed.

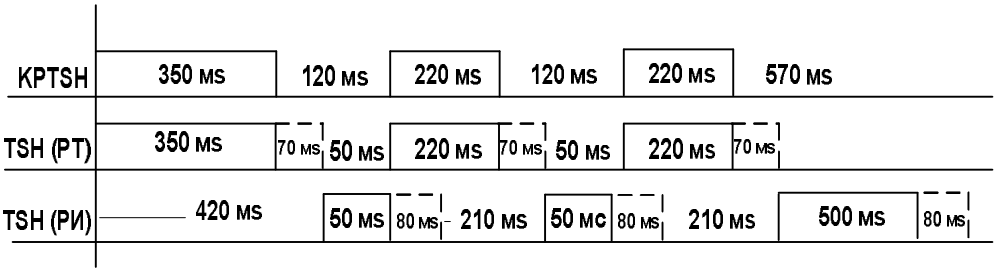

Figure 12. Diagram of the timing characteristics of pulse intervals in the code «G» for relay-transmitters TSH-65 and TSH-2000.

Table 1 lists the processes and descriptions of processes in Petri nets for code «G»

Table 1

Order of proceedings	**Purpose of the procedure**
P1	The supply was given and the impulse started to come.
P2	Dropping of PT relay armature .
P3	The process of checking the arrival of a pulse for 350 MS (milliseconds).
P4	PT relay anchor drops during the interval after the pulse ends expiration of the delay time in 70 MS.
P11	
P15	
P5	During the pulse, the process of raising the armature of the PT relay.
P6	Interval process for 50 MS.
P12	
P7	Dropping of РИ relay anchor.
P8	80MS delay time for pulse arrival and РИ relay armature drop out after interval timeout check process.
P13	
P17	
P9	Pulse arrival and РИ relay armature delay of 80 MS and pulse arrival process of 220 MS.
P14	
P10	The rise of РИ relay armature.
P16	Interval arrival process for 500 MS
Order of conditions	**Assigning transition conditions**
t1	Start receiving pulse 0÷350MS
t2	Checking the transition condition to the interval after the end of the impulse.
t6	
t10	
t3	After the 70 MS delay, the armature of the PT relay switches from the energized state to the de-energized state.
t7	
t11	
t4	Checking of the 50 MS interval continues after the 70 MS delay time.
t8	
t5	Checking the start of the 80 MS delay after the 50 MS interval.
t9	
t12	Checking of the 500 MS interval comes after the 70 MS delay.
t13	Checking of 80MS delay timeout and RI relay switching to no current state.

The graph consists of transitions t1, t2, ... and t22 and processes P1, P2 ..... and P17.

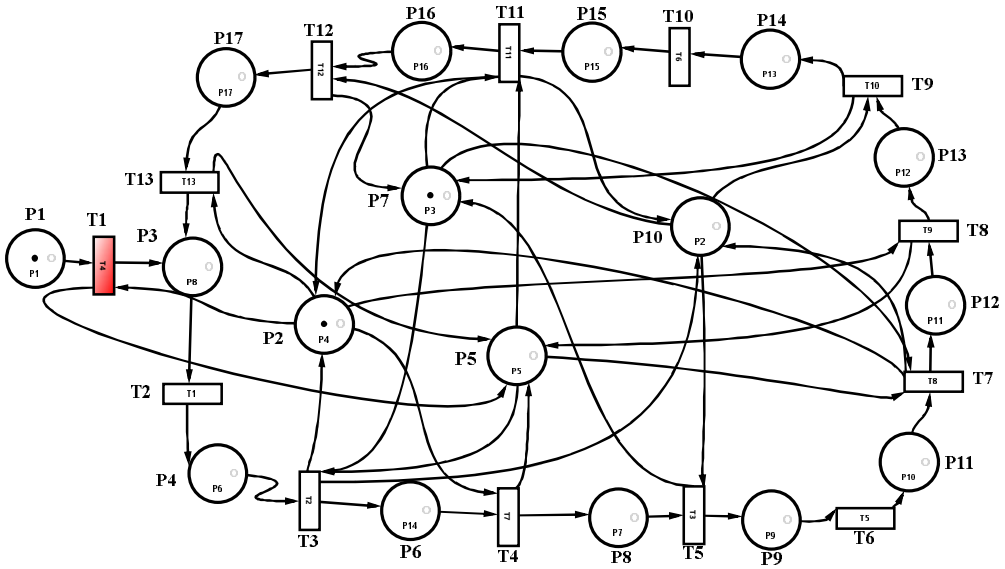

Figure 13. «G» code TSH transmitter relays start state when supply is connected Graph representation of Petri net

A power-on pulse activates process P1. As a result of the fulfillment of the condition for the arrival of a pulse for a period t1 350 MS, we obtain outputs O(t1) = {P3, P5} (Fig. 13).

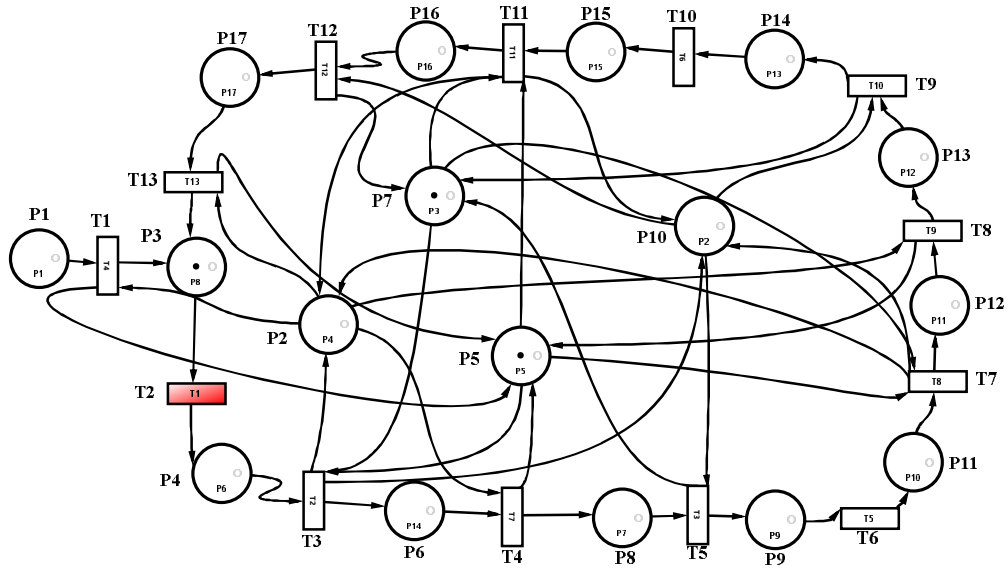

Figure 14. TSH transmitter relays for «G» code when the power supply is connected 0÷350 MS pulse receiving state representation of the Petri net graph.

Outputs O(t1) = {P3, P5} activate the processes shown in Figure 14. Process P3 is used to transfer the armature of the relay PT to the current state as a result of the condition t1. And the P5 process controls the process of the pulse input to the PT armature for 0÷350 MS. 350 MS after the input of the pulse on arrival, I(t2)={P4} checks the condition for the beginning of the interval after the end of the input pulse (Figure 14).

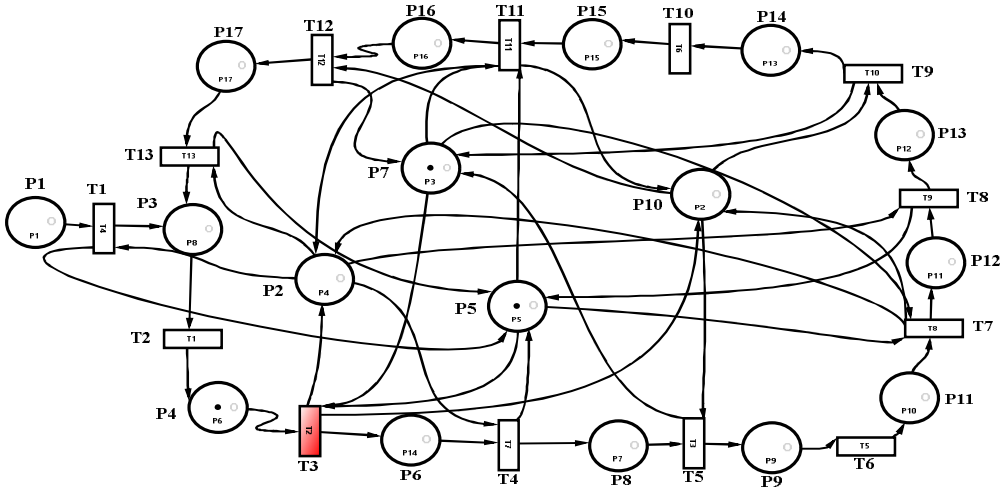

Figure 15. Petri net plot of 70MS delay process testing PT anchor drop for code «G».

Figure 15 shows that the delay time of 70 MS for the execution of the input data I(t3)={P6,P10} to release the PT armature due to the activation of the P4 process has ended.

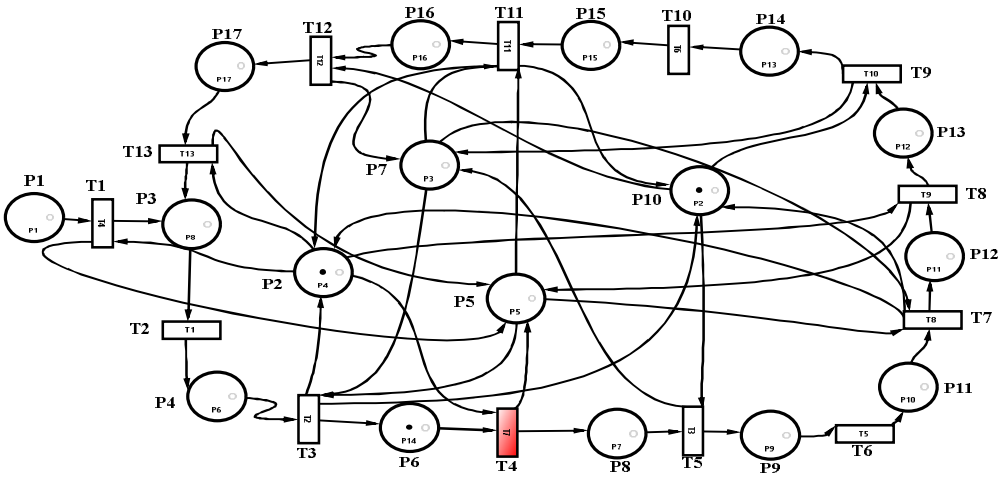

Figure 16. Petri net plot of PT anchor drop and 50 MS interval for code “G”.

In Figure 16, generating output O(t3)={P2} results in a token in process P2, which represents the fall of the PT armature. O(t3)={P6} passes through the chip to process P6. And in this process there is a time interval of 50 ms.

A total of 120 ms of latency and interval time ensures that the interval is fully implemented. The end of the interval sets the stage for the start of the next impulse process via the output O(t4)={P5}(Fig. 6).

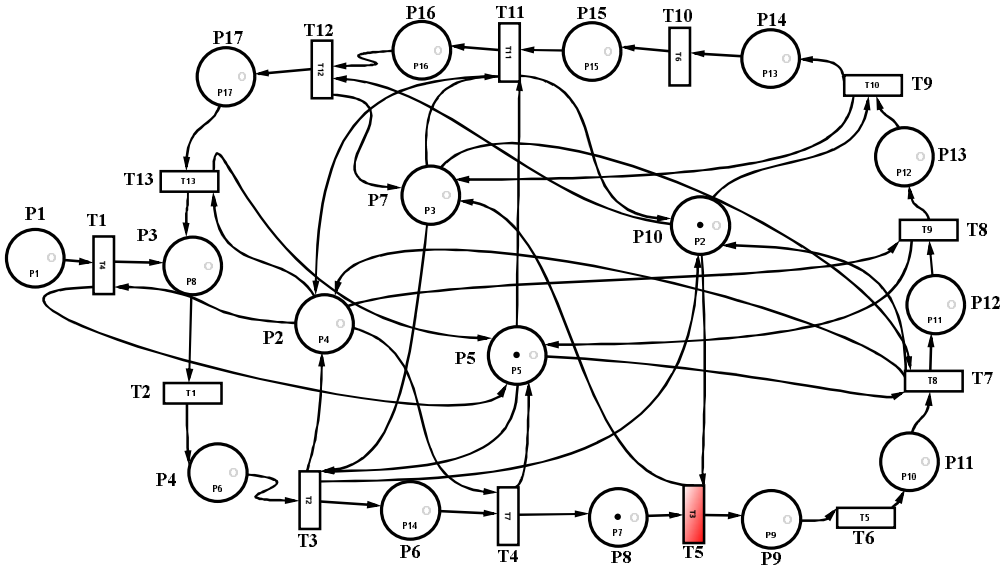

Figure 17. РИ anchor rise for «G» code Petri net graph

When O(t4)={P8} output occurs, the t5 condition controls the interval and the 80MS interval delay start condition. After that, process P7 and P9 is activated with output O(t5)={P7,P9}. The appearance of a microcircuit on P9 starts the process of entering a pulse for 220 MS (Fig. 17).

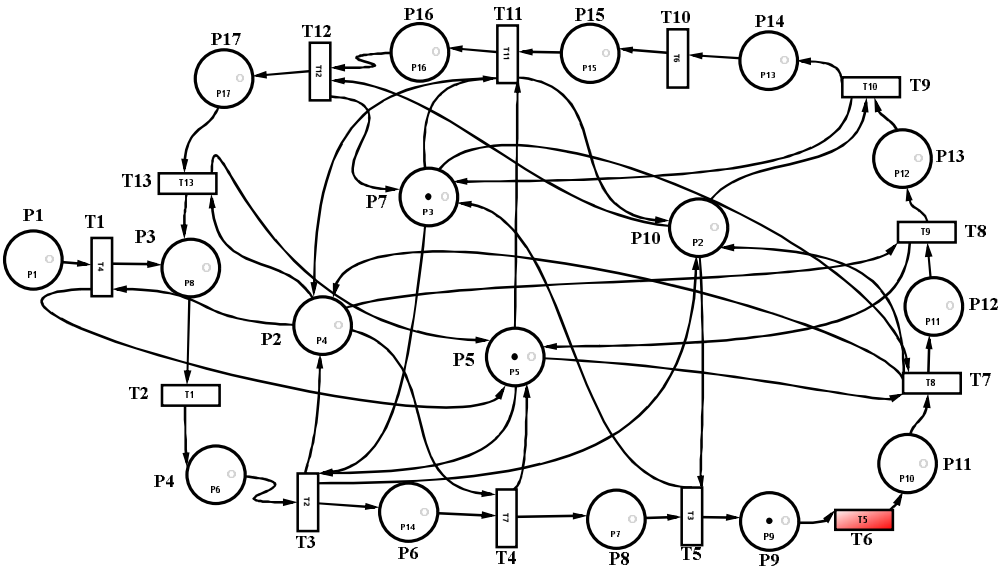

Figure 18. Delay time for РИ anchor drop for «G» code Petri net graph

Figure 18 shows the process of fulfilling the condition of the delay time for the РИ anchor to drop as a result of the activation of the process P7 through the input I(t6)={P9}.The presence of input data I(t5)={P8,P10} indicates that the delay of 80 MS has ended. The fulfillment of the condition t8 activates the process P9, the appearance of a flash in the process P9 is considered evidence that the armature РИ has passed from the on state to the de-energized state. Therefore, the first impulse and the interval come to an end. O(t4)={P8} indicates that the second pulse has started.

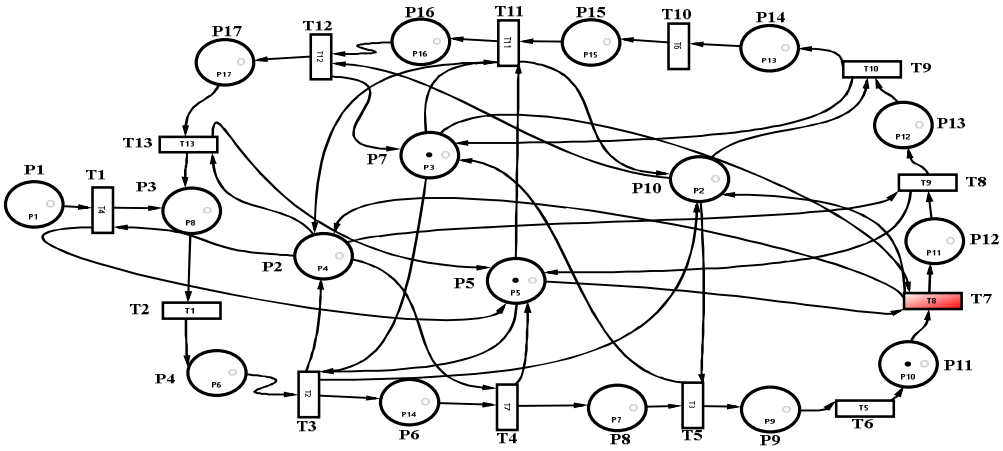

Figure 19. Graph of the Petri net showing the beginning of the 2nd cycle and the arrival of the pulse between 470 ÷ 690 MS for code «G»

The activation of process P11 indicates that the reception of pulses has begun. Activation of the P12 process serves to lift the PT anchor. The transition of the PT armature to the current state is a process of an incoming pulse with a duration of 220 MS (Fig. 19).

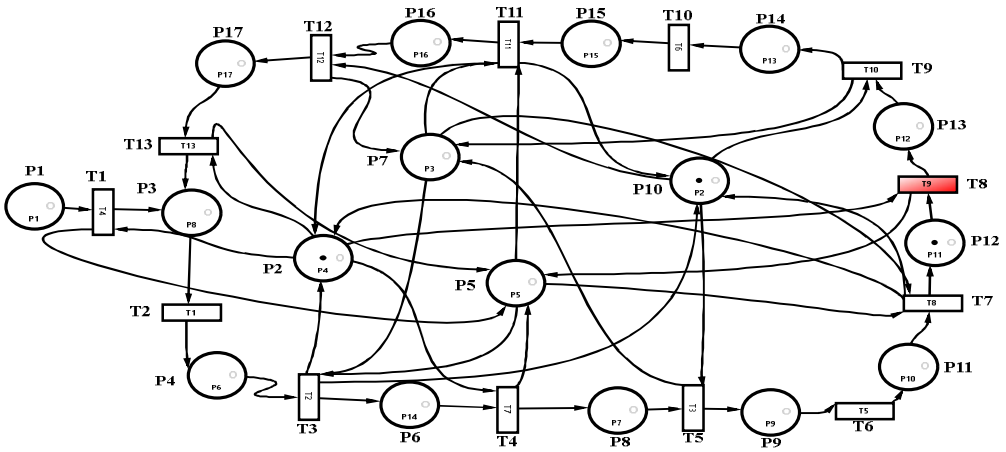

Figure 20. Plot of the Petri net of the transition of the PT armature from the energized state to the de-energized state for code «G».

In Figure 9, output O(t6)={P11} is generated and P11 is activated. As a result, the PT lowers the anchor. The transition of the PT from the on state to the de-energized state means the end of the pulse in the second cycle. Activating P12 causes the interval to last 50 ms and input I(t8)={P12}.

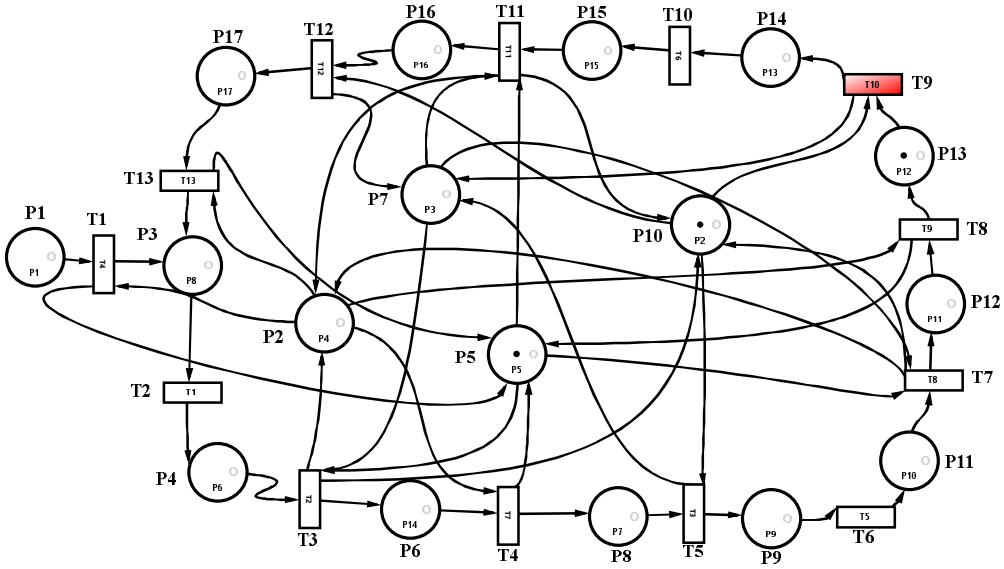

Figure 21. Petri net plot of РИ anchor transition from dead to live for G code.

Generation of output data O(t7)={P10} serves to raise the РИ anchor. And the input I(t8)={P12} checks the interval condition for 50 MS(Figure 21).

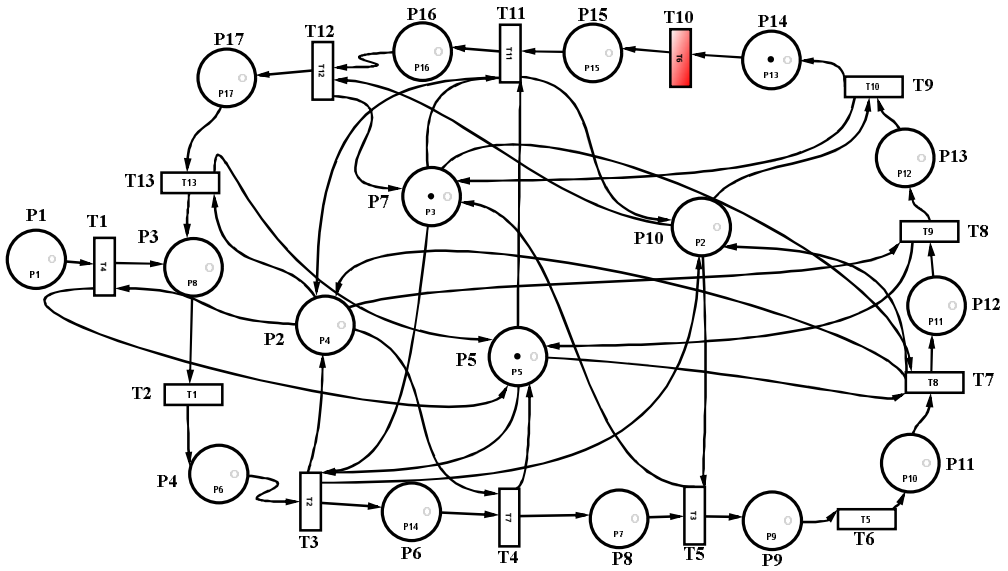

Figure 22. Petri net plot of the current to uncurrent РИ anchor transition for code «G».

Figure 22 illustrates the 80MS delay that goes into lowering the РИ anchor in process P16 via output O(t8)={P13}.The execution of this process generates the input I(t9)={P10,P13} and checks the conditions for the transition of the t9 РИ armature from the on state to the de-energized state. Therefore, after the interval and delay time has elapsed, process P7 is activated, and the switchgear armature goes into the open state. Therefore, the second impulse and the interval come to an end.

The appearance of the output O(t8)={P13} means that the process of the third impulse has begun. The chip appears in the process P14 through the output O(t9)={P14}.

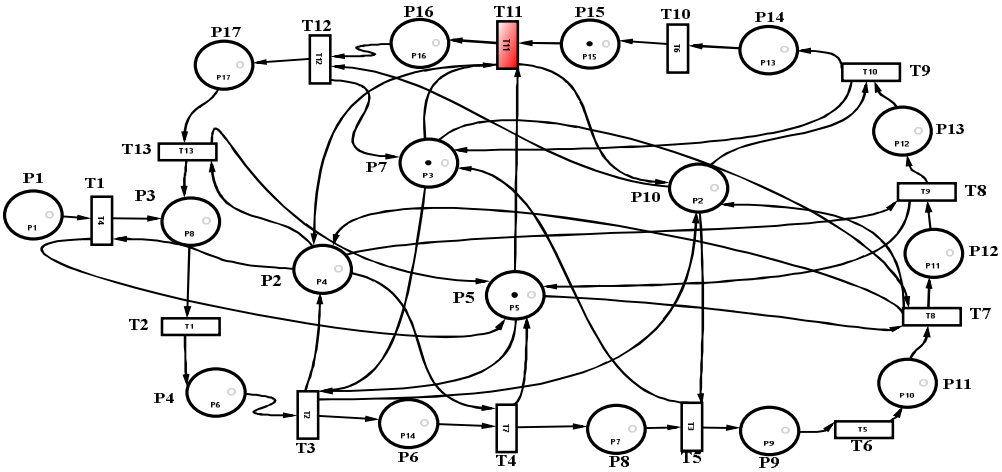

Figure 23. Petri net graph of pulse arrival for 810÷1030 MS for «G» code.

O(t9)= {P14} in process P14 via output 810÷1030 MS interval indicates that the pulse is present. (t10)={P15} outputs a 70ms delay to drop the RT anchor in process P15. (Fig. 23).

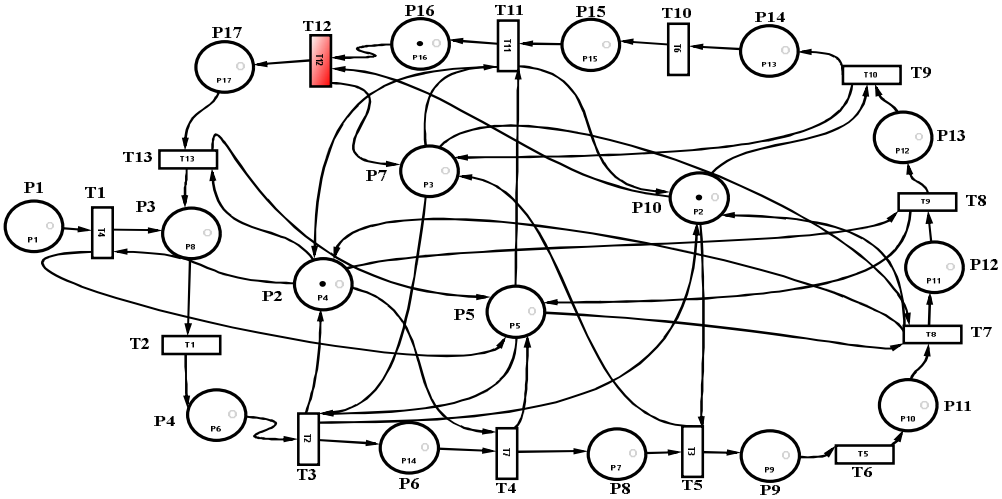

Figure 24. Plot of the Petri net of the transition of the PT anchor from on to off for the code «G»

After checking that the impulse came completely through the conditional t11, we get the input I(t11)={P5,P15}. This, in turn, activates process P2 to switch the armature PT from the on state to the de-energized state. Through the output O(t11)={P16} in the process P16, the interval of 500 MS begins (fig. 24).

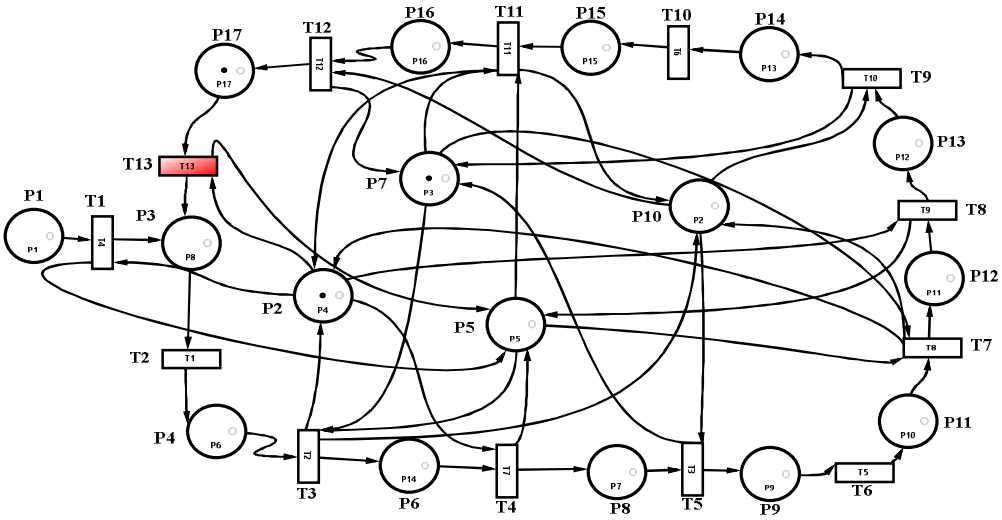

Figure 25. Graph of the Petri net of the transition of the РИ armature from a de-energized state to on for the code «G»

Figure 25 shows the transition to the current state due to the rise of the armature РИ in the process of P10 through the output O(t11)={P10}.As a result of exit O(t11)={P16} process P16 is activated represented by interval 1100÷1600 MS.

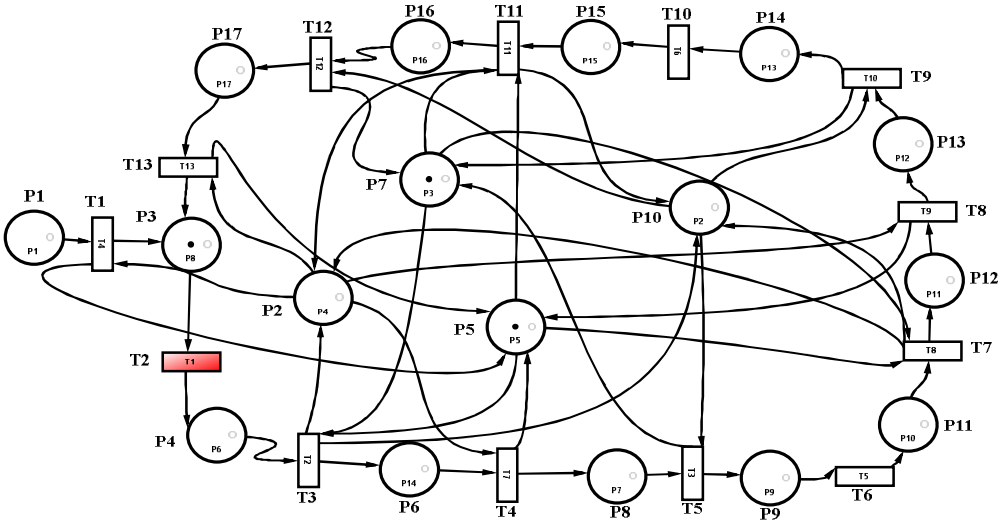

Figure 26. Plot of the Petri net after three impulses and three intervals for the code «G».

The appearance of the inputs I(t13)={P17,P10} activates the check of the end of the interval and return to the initial state. O(t13)={P3} activates process P3 via exit. Which, in turn, is equal to 0÷350. When organizing the arrival of through the impulses and intervals for the code «G» mean that the sequence of arrivals starts again from the beginning of Fig. 26 .

The fulfillment of the condition t12 leads to the output O(t22)={P7} in addition to the output O(t12)={P17}. As a result, the P17 process is activated, and after the delay time of 80 MS for the fall of the РИ armature, the РИ armature is de-energized, thereby completing the third interval .

Extended input (I) and output (O) functions for the Petri graph in the code «G» of the TSH-65 relay are presented in Table 4.

table 4

I(t1)={P1,P5}	*O(t1)={P3,P5}*
I(t2)={P3}	*O(t2)={P4}*
I(t3)={P4,P5,P7}	*O(t3)={P2,P6,P10}*
I(t4)={P2,P4}	*O(t4)={P5,P8}*
I(t5)={P8,P10}	*O(t5)={P7,P9}*
I(t6)={P9}	*O(t6)={P11}*
I(t7)={P5,P7,P11}	*O(t7)={P2,P10,P12}*
I(t8)={P2,P12}	*O(t8)={P5,P13}*
I(t9)={P10,P13}	*O(t9)={P7,P14}*
I(t10)={P14 }	*O(t10)={P15}*
I(t11)={ P5,P7,P15 }	*O(t11)={P2,P10,P16}*
I(t12)={P10,P16}	*O(t12)={P7,P17}*
I(t13)={P12,P17}	*O(t13)={P3,P5}*

Corresponding to the expression in Table 2, the expression forms a matrix of shapes 3 and 4.

$$i_{j\varepsilon} = \begin{cases} 1, agar \rightarrow p_\varepsilon \in P^I t_j \cup t_j \in T^0 p_\varepsilon, \\ 0, agar \rightarrow p_\varepsilon \notin P^I t_j \cap t_j \notin T^0 p_\varepsilon \end{cases}$$

Matrix 3

$I=|t_{\tau\varepsilon}|=$

P1	P2	P3	P4	P5	P6	P7	P8	P9	P10	P11	P12	P13	P14	P15	P16	P17	
0	0	0	0	0	0	0	0	0	0	0	0	0	0	0	0	0	t1
0	0	0	0	0	0	0	0	0	0	0	0	0	0	0	0	0	t2
0	0	0	0	0	0	0	0	0	0	0	0	0	0	0	0	0	t3
0	0	0	0	0	0	0	0	0	0	0	0	0	0	0	0	0	t4
0	0	0	0	0	0	0	0	0	0	0	0	0	0	0	0	0	t5
0	0	0	0	0	0	0	0	0	0	0	0	0	0	0	0	0	t6
0	0	0	0	0	0	0	0	0	0	0	0	0	0	0	0	0	t7
0	0	0	0	0	0	0	0	0	0	0	0	0	0	0	0	0	t8
0	0	0	0	0	0	0	0	0	0	0	0	0	0	0	0	0	t9
0	0	0	0	0	0	0	0	0	0	0	0	0	0	0	0	0	t10
0	0	0	0	0	0	0	0	0	0	0	0	0	0	0	0	0	t11
0	0	0	0	0	0	0	0	0	0	0	0	0	0	0	0	0	t12
0	0	0	0	0	0	0	0	0	0	0	0	0	0	0	0	0	t13

Matrix 4

$O=|t_{\tau\varepsilon}|=$

P1	P2	P3	P4	P5	P6	P7	P8	P9	P10	P11	P12	P13	P14	P15	P16	P17	
0	0	0	0	0	0	0	0	0	0	0	0	0	0	0	0	0	t1
0	0	0	0	0	0	0	0	0	0	0	0	0	0	0	0	0	t2
0	0	0	0	0	0	0	0	0	0	0	0	0	0	0	0	0	t3
0	0	0	0	0	0	0	0	0	0	0	0	0	0	0	0	0	t4
0	0	0	0	0	0	0	0	0	0	0	0	0	0	0	0	0	t5
0	0	0	0	0	0	0	0	0	0	0	0	0	0	0	0	0	t6
0	0	0	0	0	0	0	0	0	0	0	0	0	0	0	0	0	t7
0	0	0	0	0	0	0	0	0	0	0	0	0	0	0	0	0	t8
0	0	0	0	0	0	0	0	0	0	0	0	0	0	0	0	0	t9
0	0	0	0	0	0	0	0	0	0	0	0	0	0	0	0	0	t10
0	0	0	0	0	0	0	0	0	0	0	0	0	0	0	0	0	t11
0	0	0	0	0	0	0	0	0	0	0	0	0	0	0	0	0	t12
0	0	0	0	0	0	0	0	0	0	0	0	0	0	0	0	0	t13

Conclusion

In the field of automation and telemechanics of Joint Stock Company «Uzbekistan Temir Yollari « in the field of autoblocking and automatic locomotive signaling, the Petri graphs of the integrated microelectronic code transmitter device, which are proposed to be used instead of TSH-65 and TSH-2000 relays, which serve to transmit the codes generated by the KPTSH relay to the locomotive traffic lights or road traffic lights, are based on «Y ” was modeled for the code. As a result, it is recommended to abandon contact devices and use a new type of microelectronic device.

In the field of railway automation and telemechanics, code transmitting devices are modeled on the basis of Petri nets, and the processes occurring in the delivery of existing «G» codes in sections equipped with autoblocking and automatic locomotive signaling are described by the example of Petri graphs. Each described process was studied in the Petri Mathematical Simulator.

Used Literature

1. Soroko V. I., Fotkina Zh. V. Equipment for railway automatics and telemechanics: Reference book: in 4 books. Book. 1. - 4th ed. - M .: LLC «NPF» PLANET «, 2013 - 1060 p.
2. Kazanov A. A. et al. Systems of interval regulation of train traffic / A. A. Kazakov, V. D. Bubnov, E. A. Kazakov: A textbook for railway technical schools. transp. — M.: Transport, 1986. — 399 p.
3. Kazakov A.A., Bubnov V.D., Kazakov E.A. Automated systems for interval control of train traffic: Textbook, for technical schools of the railway. transp. M.: Transport, 1995. - 320 p.
4. Theeg G., and Vlasenko S. «Railway Signaling & Interlocking - International Compendium», Eurailpress, 2009, 448 p.
5. Saitov, A., Kurbanov, J., Toshboyev, Z., & Boltayev, S. (2021). Improvement of control devices for road sections of railway automation and telemechanics. E3S Web of Conferences, 264, 05031. doi:10.1051/e3sconf/202126405031.
6. Azizov, A.R., & Shakirova, F.F. (2020). Method for assessing the diagnosis of the technical condition of an integrated microprocessor pulse generator of railway automation and telemechanics. In IOP Conference Series: Materials Science and Engineering (Vol. 862). Institute of Physics Publishing.https://doi.org/10.1088/1757-899X/862/5/052073
7. Sapozhnikov V.V., Sapozhnikov Vl.V., Efanov D.V., Nikitin D.A. «Berger code generation method with increased efficiency of error detection in data bits» // Electronic Modeling, 2013, vol. 1, p. 35, no. 4, pp. 21-34.
8. Boltayev S.T., Gayubov T.N., Rakhmonov B.B., Kosimova Q.A., Ergashov B.G. The creation of microprocessor controlled modules for AC and DC conductors. Journal of critical reviews (JCR), 2020, 7(17): 2183-2189. 10.31838/jcr.07.17.268
9. S. Boltayev, B.Rakhmonov, O.Muhiddinov, A.Saitov, Z.Toshboyev A block model development for intelligent control of the switches operating apparatus position in the electrical interlocking system. CONMECHYDRO – 2021 E3S Web of Conferences 264, 05043 (2021) https://doi.org/10.1051/e3sconf/202126405043
10. Boltayev S.T., Valiyev S.I., Qosimova Q.A. Improving the Method of Sending Information about the Approach of Trains to Railway Crossings. St. Petersburg Electrotechnical University “LETI”, and IEEE Russia North West Section Conference of Russian Young Researchers in Electrical and Electronic Engineering

(ElConRus) January 25 - 28, 2022 St. Petersburg, Russia. -Electronic ISBN:978-1-6654-0993-3 CD:978-1-6654-0992-6 Print on Demand(PoD) ISBN:978-1-6654-0994-0, 2022-yil. DOI: 10.1109/ElConRus54750.2022.9755564

11. Boltayev S.T., Abdullaev R.B., Ergashov B.G., Hasanov B.Q. Simulation of a Safe Train Traffic Management System at the Stations. St. Petersburg Electrotechnical University "LETI", and IEEE Russia North West Section Conference of Russian Young Researchers in Electrical and Electronic Engineering (ElConRus) January 25 - 28, 2022 St. Petersburg, Russia. -Electronic ISBN:978-1-6654-0993-3 CD:978-1-6654-0992-6 Print on Demand(PoD) ISBN:978-1-6654-0994-0, 2022-yil. DOI: 10.1109/ElConRus54750.2022.9755616
12. Sapozhnikov V., Sapozhnikov V., Efanov D. and Nikitin D., «Combinational circuits checking on the base of sum codes with one weighted data bit,» Proceedings of IEEE East-West Design & Test Symposium (EWDTS 2014), 2014, pp. 1-9, doi: 10.1109/EWDTS.2014.7027064.
13. https://elektrikexpert.ru/tverdotelnoe-rele.html.
14. Bose, B., & Lin, DJ (1985). Systematic Unidirectional Error-Detecting Codes. IEEE Transactions on Computers, C-34(11), 1026-1032.https://doi.org/10.1109/TC.1985.1676535
15. Fujiwara, E. (2005). Code Design for Dependable Systems: Theory and Practical Applications. Code Design for Dependable Systems: Theory and Practical Applications (pp. 1–701). John Wiley and Sons.https://doi.org/10.1002/0471792748
16. Hololobova, O., Buriak, S., Havryliuk, V., Skovron, I., & Nazarov, O. (2019). Mathematical modeling of the communication channel between the rail circuit and the inputs devices of automatic locomotive signalization. MATEC Web of Conferences, 294, 03009.https://doi.org/10.1051/matecconf/201929403009
17. Peterson J. Theory of Petri nets and system modeling per:, per.ang. - M.: 1984. - 264 p..
18. Aripov N.M., Mirzarakhmedov Z.F. "MODELING OF CODE TRANSMISSION PROCESS OF MICROELECTRONIC TRANSMITTER RELAYS" Europen Journal of Research Development and Sustainability (EJRDS) № 9 September 2022. C 77-87. https://scholarzest.com/index.php/ejrds/article/view/2700
19. Aripov N.M., Mirzarakhmedov Z.F., Rakhmonov B.B, Qosimova Q.A. "DEVELOPMENT OF A MICROELECTRONIC CONVERTER FOR RAILWAY AUTOMATION AND TELEMECHANICAL SYSTEMS" Journal of Hunan University (Natural Sciences)" VOL.49 №08. Avgust 2022. 1040-1046. https://johuns.net/index.php/publishing/410.pdf
20. Mirzarakhmedov Z.F. "MATHEMATICAL MODELING OF MICROELECTRONIC TRANSMITTERS USING PETRI NET" Spectrum Journal of Innovation, Reforms and Development № 07 29.09.2022 c 116-125.https://www.sjird.journalspark.org/index.php/sjird/article/view/247/.